Three-dimensional numerical modeling of bottom-diffracted surface-reflected arrivals in the North Pacific

R.A. Stephen[1], I.A. Udovydchenkov[1], S.T. Bolmer[1], D. Komatitsch[2], J. Tromp[3], E. Casarotti[4], Z. Xie[2], and P.F. Worcester[5]

1 - Woods Hole Oceanographic Institution, Woods Hole, MA, 2 - CNRS, Laboratory of Mechanics and Acoustics, Marseille, 3 - Princeton University, Princeton, NJ, 4 - National Institute of Geophysics and Volcanology, Rome, 5 - Scripps Institution of Oceanography, La Jolla, CA

S23C-2747

0) ABSTRACT

Bottom-diffracted surface-reflected (BDSR) arrivals were first identified in the 2004 Long-range Ocean Acoustic Propagation Experiment (Stephen et al, 2013, JASA, v.134, p.3307-3317). The BDSR mechanism provides a means for acoustic signals and noise from distant sources to appear with significant strength on the deep seafloor. At depths deeper than the conjugate depth ambient noise and PE- predicted arrivals are sufficiently quiet that BDSR paths, scattered from small seamounts, can be the largest amplitude arrivals observed. The Ocean Bottom Seismometer Augmentation in the North Pacific (OBSANP) Experiment in June-July 2013 was designed to further define the characteristics of the BDSRs and to understand the conditions under which BDSRs are excited and propagate. The reciprocal of the BDSR mechanism also plays a role in T-phase excitation. To further understand the BDSR mechanism, the SPECFEM3D code was extended to handle high-frequency, deep water bottom scattering problems with actual bathymetry and a typical sound speed profile in the water column. The model size is 38km x 27km x 6.5km. The source is centered at 10Hz with a 5Hz bandwidth. Work supported by NSF and ONR.

1) Motivation

a) BDSRs are the largest arrivals on deep seafloor receivers

On NPAL04 Bottom-Diffracted Surface-Reflected (BDSR) arrivals were the largest amplitude arrivals observed on the vertical component of the OBSs in deep water for ranges from 250 to 3200km. [Stephen et al, 2009; 2013]

BDSR arrivals are like a palimpsest. They are present throughout the water column, but at depths above the conjugate depth they are obscured by ambient noise and PE predicted arrivals.

The hypothesis is that BDSR paths contribute to the arrival structure on the deep seafloor at all ranges from near zero range to 4-1/2CZs.

The questions are: 1) What are the characteristics of BDSR paths (eg. sensitivity to angle in the azimuthal and sagittal planes)? 2) What are the characteristics of the seafloor features that are responsible for BDSR paths?

b) BDSRs are the reciprocal of T-phase excitation problem

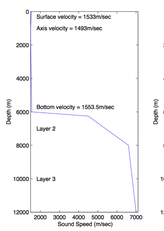

Figure 1: Many T-phases are excited by earthquakes occuring beneath an ocean that is deeper than the conjugate depth. Ray paths from sources in the high velocity crust are too steep (low incident angles) to couple into the sound channel. Sound channel propagation requires flatter (high incident angle) rays.

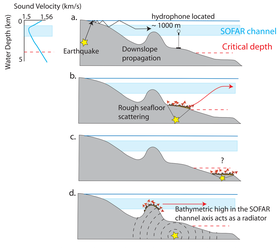

Figure 2: Illustrations of coupling mehanisms that generate T-phases. (a) Downslope propagation and (b) rough seafloor scattering. (c) Events that occur below the critical depth should not be able to propagate in the SOFAR channel based on ray trace theory. (d) A local bathymetric high located in the SOFAR channel axis may act as a radiator, where acoustic energy from a deep water event enters the SOFAR channel efficiently and results in T-phase event locations that are not epicenters. BDSRs are the reciprocal of mechanisms c and d.

2) NPAL04

Bottom-diffracted surface-reflected arrivals were first identified on the North Pacific Acoustic Laboratory (NPAL) experiment in 2004 for ranges from 500 to 3200km.

a) Source and Receiver Locations

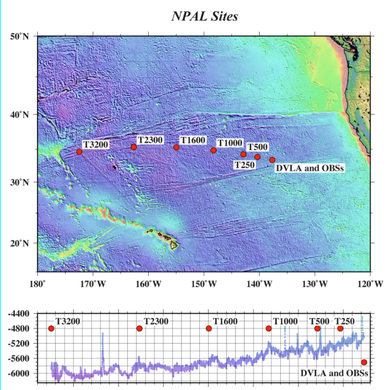

Figure 3: Water depth for the propagation paths on NPAL04 was deeper than 4400m. The long range transmissions were observed on the Deep Vertical Line Array (DVLA) and three Ocean Bottom Seismometers (OBSs). Deepest DVLA element was 750m above the OBSs on the seafloor at ~5,000m.

b) Bottom-Diffracted Surface-Reflected (BDSR) Arrivals

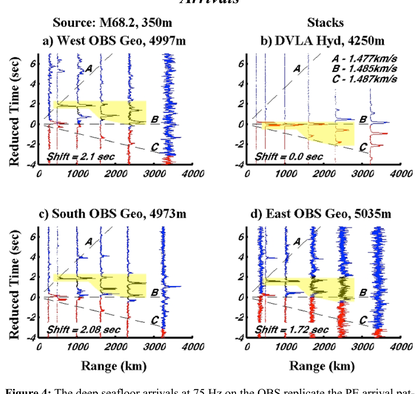

Figure 4: The deep seafloor arrivals at 75 Hz on the OBS replicate the PE arrival pattern on the deepest element of the DVLA. The shifts of these seafloor arrivals with respect to the PE arrival on the DVLA are constant regardless of range!!! It is remarkable how robust and simple this pattern is. Deep seafloor arrivals are "not" random!

c) Bottom-Diffracted Surface-Reflected Arrivals from a Seamount on NPAL04

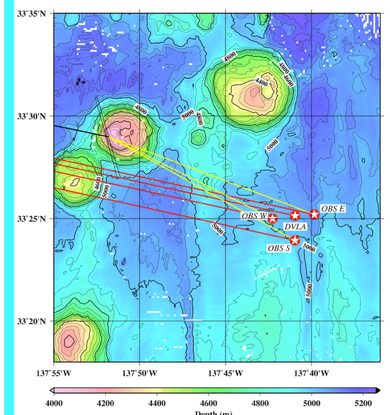

Figure 5i:

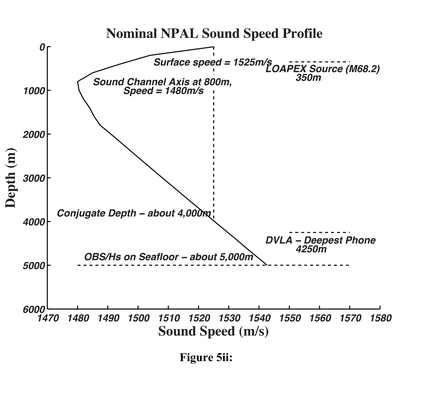

Figure 5ii:

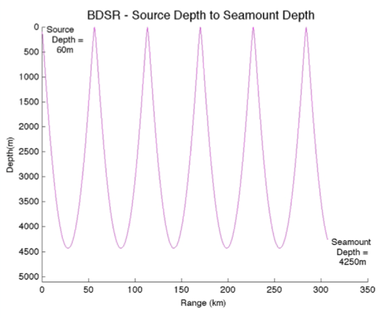

Figure 5iii:

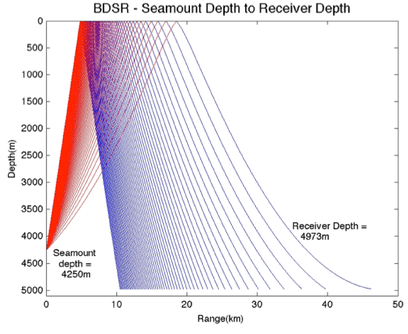

Figure 5iv:

Figure 5: The bottom-diffracted surface-reflected arrivals in Figure 4 were scattered from the top of the seamount shown in 5i). The black path in 5i) indicates the sound channel propagation path that is shown schematically in 5iii) based on the sound speed profile in 5ii). The yellow paths from the seamount to the receivers in 5i) are the surface reflected path as shown schematically in 5iv).

3) OBSANP

The NPAL04 site was revisited on the Ocean Bottom Seismometer Augmentation in the North Pacific (OBSANP) Experiment in 2013 to study the BDSR mechanism in more detail. BDSRs were observed at ranges from 10 to 40km.

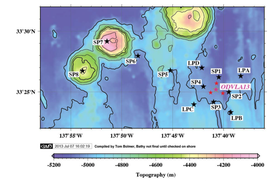

Figure 6: Locations of the eight short period OBSs (SP*), the four long period OBSs (LP*), and the OBSANP DVLA (ODVLA13) with respect to the bathymetric relief. The three red stars around ODVLA13 are the acoustic transponders used to measure mooring motion.

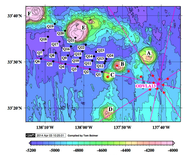

Figure 10: A "pin cushion" of station stops was designed to ensonify Seamounts B and C at a variety of sagittal and azimuthal angles. The stations span 1/2 CZ from the O-DVLA and the seamounts. Q1 to Q6 are on the LOAPEX (NPAL04) geodesic. Q13 to Q18 are collinear with Seamount B and the O-DVLA. Q7 to Q12 and Q19 to Q24 are aligned with Seamount B but are oblique to the ODVLA13 transmission path. The red stars are the locations of the OBSs. The magenta lines show the locations of the short-range tows.

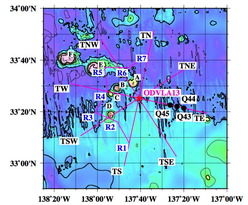

Figure 7: Phase 3 of the transmission program carried out a comprehensive survey of radial lines out to 50 km and half of a Star of David pattern spanning 1/2CZ from the DVLA .

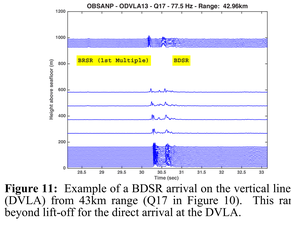

Figure 11: Example of a BDSR arrival on the vertical line array (DVLA) from 43km range (Q17 in Figure 10). This range is beyond lift-off for the direct arrival at the DVLA.

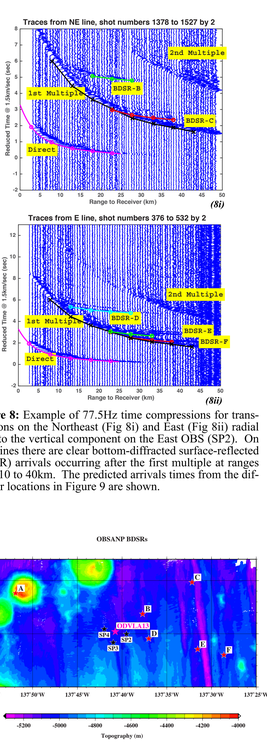

Figure 8: Example of 77.5Hz time compressions for transmissions on the Northeast (Fig 8i) and East (Fig 8ii) radial lines to the vertical component on the East OBS (SP2). On both lines there are clear bottom-diffracted surface-reflected (BDSR) arrivals occurring after the first multiple at ranges from 10 to 40km. The predicted arrivals times from the diffractor locations in Figure 9 are shown.

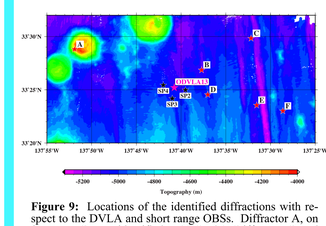

Figure 9: Locations of the identified diffractions with respect to the DVLA and short range OBSs. Diffractor A, on Seamount B, was identified on NPLA04. Diffractors B and C are identified on the Northeast line to the East OBS (SP2-E) (Figure 8i). Diffractors D, E and F are identified on the East line to the East OBS (Figure 8ii). Note that diffractors B through F are not associated with any noticeable bathymetric features.

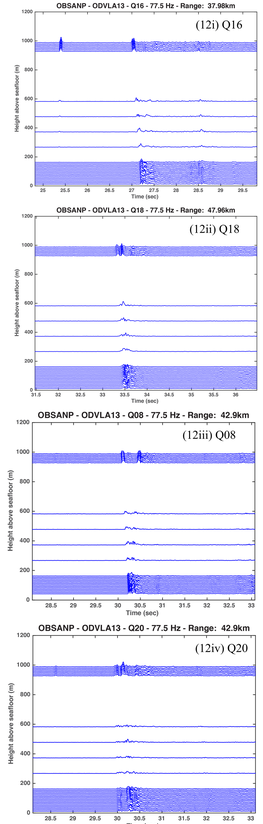

Figure 12: Arrival structure at the neighboring Q-stops to Q17 in Figure 11. See Figure 10 for locations. The clear separation of BRSR and BDSR at Q17 is less distinct at the neighboring stations. This indicates the sensitivity of diffracted energy to azimuthal and sagittal incident angles.

4) SPECFEM3D

The SPECFEM3D method is being used to model the BDSR mechanism. First we needed to introduce separate attenuation mechanisms for compressional and shear waves, we needed to improve the absorbing boundaries, and we needed to compare SPECFEM3D results with other methods such as the parabolic equation method for range independent environments.

Spectral Finite-Element Model SPECFEM3D

- 3D model.
- Finite-element (time domain).
- Solves equations of motion in the weak form (integrated momentum equation with stress-free boundary condition at the earth's surface and absorbing boundary condition at other model boundaries).
- Supports environments with rigidity.
- Supports all interactions between body waves, interface waves (Rayleigh and Stoneley) and guided waves (modes and T-phases).
- Allows heterogeneities at the sub-wavelength scale.
- Designed for parallel computations on a cluster or a supercomputer.

Some problems in marine seismology that would benefit from modeling with SPECFEM3D

- Excitation of Earth's hum by surface- gravity wave loading on coastlines. (0.001-0.03 Hz)
- Inferring crustal rigidity from seafloor compliance. (0.001-0.03Hz)
- Ice shelf excitation by surface gravity waves. (0.01-0.1 Hz)
- The excitation and propagation of microseisms. (0.1-0.5 Hz)
- The T-phase excitation problem. (5-30 Hz)
- Interpreting 3-D multi-channel seismic data over axial magma chambers. (5-100 Hz)

SPECFEM3D vs RAM2D

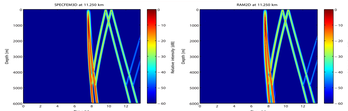

Figure 13: Wave field intensities as functions of arrival time and depth computed using SPECFEM3D (left panel) and RAM (right panel) are shown for a laterally uniform ocean with a constant depth (4950 m). A broadband acoustic source with the same characteristics as in Figure 1 is placed at 750 m depth. The bottom is homogeneous with a density of 1350 kg/m^3 and a compressional velocity of 1.6 km/s. The water column sound speed profile is similar to a "Munk-like" mid-latitude ocean profile.

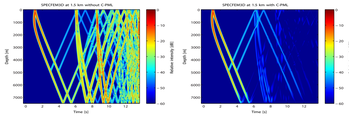

Figure 14: Wave field intensities as functions of arrival time and depth computed using SPECFEM3D without using the convolutional perfectly matched layer (C-PML) (left panel) and with C-PML are shown for a laterally uniform ocean with a constant depth (4950 m). A broadband acoustic source is placed at 750 m depth. The bottom is homogeneous with a density of 1350 kg/m^3 and a compressional velocity of 1.6 km/s. The water column sound speed profile is the same as in Figure 13.

! Reflections from Boundaries of the computational domain are efficiently attenuated with C-PML.

Estimating compressional attenuation using "spectral ratio method"

Consider a plane compressional wave, $u(x,t)$, propagating in the x direction in a homogeneous medium. This propagation is described by the well-known one dimensional wave equation

$$\rho(x)\frac{\partial^2 u(x,t)}{\partial t^2} = \frac{\partial}{\partial x}\left(M(x)\frac{\partial u(x,t)}{\partial x}\right) \quad (1)$$

where ρ is the density of the medium and M is the appropriate modulus. For strictly harmonic motion M can be replaced by the complex modulus $M^*(\omega) = \sigma(\omega)/\varepsilon(\omega)$, where σ and ε are stress and strain, respectively. A solution to Equation (1) can be written as a damped wave:

$$u(x,t;\omega) = u_0 \exp(\alpha(\omega)x)\exp(i\omega(t - x/c(\omega))), \quad (2)$$

where $\alpha(\omega)$ is the attenuation coefficient and $c(\omega)$ is the phase velocity.

The internal friction is expressed as

$$1/Q(\omega) = 2c(\omega)\alpha(\omega)/\omega \quad (3)$$

Q is obtained from impulsive source data at two receivers by the "spectral ratio method":

$$\ln\left(\left|\frac{u(x_2,\omega)}{u(x_1,\omega)}\right|\right) = -\alpha(x_2 - x_1); \alpha = \pi f/(x_2 - x_1); Q = \pi(x_2 - x_1)/(cm) \quad (4)$$

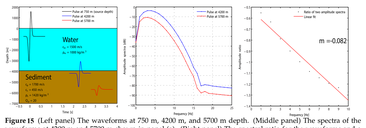

Figure 15 (Left panel) The waveforms at 750 m, 4200 m, and 5700 m depth. (Middle panel) The spectra of the waveforms at 4200 m and 5700 m shown in panel (a). (Right panel) The spectral ratio for the waveforms and a linear fit. The estimate of Q using Equations (4) based on the linear fit to the spectral ratio is 34. The input value in SPECFEM3D is 20.

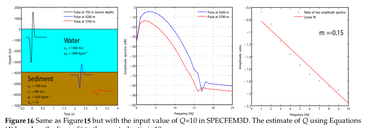

Figure 16 Same as Figure15 but with the input value of Q=10 in SPECFEM3D. The estimate of Q using Equations (4) based on the linear fit to the spectral ratio is 19.

5) Conclusions

1) BDSR arrivals have been observed at the OBSANP site at ranges less than 500m on both Ocean Bottom Seismometers and the vertical line array. They appear to be a ubiquitous feature of ocean acoustic propagation.
2) BDSR diffraction sites are not limited to the tops of seamounts. They can also occur in relatively benign abyssal plain environments.
3) SPECFEM3D is a fast and accurate method for computing 3-D seismic wavefields in media with fluid-solid interfaces. The SPECFEM3D method includes all compressional, shear, interface and evanescent wave effects as well as scattering from both bottom roughness and volume heterogeneity.
4) Reflections from boundaries of the computational domain are efficiently attenuated with C-PML.
5) The validity of SPECFEM3D results for ocean acoustic problems with bottom interaction has been confirmed by comparing results with parabolic equation codes.
6) Intrinsic attenuation has been introduced into SPECFEM3D for the water, soft sediments and upper oceanic crust at relatively high frequencies (1-10Hz).
7) To model the "OBSANP problem" outlined in the abstract the model needs to break the 32 bit (or 2 GB) barrier. Codes xdecompose, SCOTCH, xgenerate, and xspecfem3d need revision. In addition, the memory requirements grow so rapidly that it is unlikely that the WHOI cluster will be sufficient.
8) The BDSR arrivals observed on NPAL04 are an example of "out-of-plane" scattering from wavelength scale features. To model them requires solving the three-dimensional elastic wave equation.

6) Acknowledgements

The data acquisition was funded by the Office of Naval Research and the computer modeling using SPECFEM3D was supported by the National Science Foundation. The SPECFEM3D code was made available through the NSF funded program, Computational Infrastructure for Geodynamics. The data used in this research was provided by instruments from the Ocean Bottom Seismograph Instrument Pool (http://www.obsip.org).

7) References

Araki, E., Stephen, R. A., Shinohara, M., Kanazawa, T., and Suyehiro, K. (2004). "T-phase observed at deep seafloor boreholes," in Proceedings, Seismo-Acoustic Applications in Marine Geology and Geophysics Workshop, Woods Hole Oceanographic Institution, 24-26 March 2004, edited by Odom, R. I. and Stephen, R. A., (Applied Physics Laboratory, University of Washington, Seattle, WA.

Butler, R. (2004). "Seismoacoustic T waves at and below the sea floor," in Proceedings, Seismo-Acoustic Applications in Marine Geology and Geophysics Workshop, Woods Hole Oceanographic Institution, 24-26 March 2004, edited by Odom, R. I. and Stephen, R. A., (Applied Physics Laboratory, University of Washington, Seattle, WA.

Butler, R., and Lomnitz, C. (2002). "Coupled seismoacoustic modes on the seafloor," Geophys. Res. Lett. 29, 10.1029/2002GL014722. 10.1029/2002GL014722.

Cristini, P., and Komatitsch, D. (2012). "Some illustrative examples of the use of a spectral-element method in ocean acoustics," J. Acoust. Soc. Am. 131, EL229-EL235.

Komatitsch, D., Barnes, C., and Tromp, J. (2000). "Wave propagation near a fluid-solid interface: A spectral-element approach," Geophysics 65, 623-631.

Komatitsch, D., and Tromp, J. (1999). "Introduction to the spectral element method for three-dimensional seismic wave propagation," Geophys. J. Int. 139, 806-822.

Komatitsch, D., and Tromp, J. (2002a). "Spectral-element simulations of global seismic wave propagation—II. Three-dimensional models, oceans, rotation and self-gravitation," Geophys. J. Int. 150, 303-318.

Komatitsch, D., and Tromp, J. (2002b). "Spectral-element simulations of global wave propagation - I. Validation," Geophys. J. Int. 149, 390-412.

Mercer, J. A., Colosi, J. A., Howe, B. M., Dzieciuch, M. A., Stephen, R., and Worcester, P. F. (2009). "LOAPEX: The long-range ocean acoustic propagation experiment," IEEE J. Ocean. Eng. 34, 1-11.

Stephen, R. A., Bolmer, S. T., Dzieciuch, M. A., Worcester, P. F., Andrew, R. K., Buck, L. J., Mercer, J. A., Colosi, J. A., and Howe, B. M. (2009). "Deep seafloor arrivals: An unexplained set of arrivals in long-range ocean acoustic propagation," J. Acoust. Soc. Am. 126, 599-606. 10.1121/1.3158826.

Stephen, R. A., Bolmer, S. T., Udovydchenkov, I., Worcester, P. F., Dzieciuch, M. A., Van Uffelen, L., Mercer, J. A., Andrew, R. K., Buck, L. J., Colosi, J. A., and Howe, B. M. (2008). "NPAL04 OBS data analysis part 1: Kinematics of deep seafloor arrivals, WHOI Technical Report 2008-03, (Woods Hole Oceanographic Institution, Woods Hole, MA). doi:10.1575/1912/2725.

Stephen, R. A., Bolmer, S. T., Udovydchenkov, I. A., Dzieciuch, M. A., Worcester, P. F., Andrew, R. K., Mercer, J. A., Colosi, J. A., and Howe, B. M. (2012a). "Analysis of deep seafloor arrivals observed on NPAL04, WHOI-2012-09, (WHOI Technical Report.

Stephen, R. A., Bolmer, S. T., Udovydchenkov, I. A., Dzieciuch, M. A., Worcester, P. F., Andrew, R. K., Mercer, J. A., Colosi, J. A., and Howe, B. M. (2013). "Deep seafloor arrivals in long range ocean acoustic propagation," J. Acoust. Soc. Am. 134, 3307-3317. 10.1121/1.4818845.

Stephen, R. A., Udovydchenkov, I. A., Bolmer, S. T., Duda, T. F., Lin, Y. T., and Peter, D. (2012b). "Three dimensional numerical modeling in marine seismology," paper presented at EarthCube End-User Workshop, Arizona State University, Tempe, Arizona, , October 29-30, 2012.

Stephen, R. A., Worcester, P. F., Udovydchenkov, I. A., Aaron, E., Bolmer, S. T., Carey, S., McPeak, S. P., Swift, S. A., and Dzieciuch, M. A. (2014). "Ocean Bottom Seismometer Augmentation in the North Pacific (OBSANP) - Cruise Report, WHOI-2014-3, (Woods Hole Oceanographic Institution, Woods Hole, MA). DOI: 10.1575/1912/7130.

Udovydchenkov, I. A., Stephen, R. A., Duda, T. F., Bolmer, S. T., Worcester, P. F., Dzieciuch, M. A., Mercer, J. A., Andrew, R. K., and Howe, B. M. (2012). "Bottom interacting sound at 50km range in a deep ocean environment," J. Acoust. Soc. Am. 132, 2224-2231.

Udovydchenkov, I. A., Stephen, R. A., Duda, T. F., Lin, Y.-T., and Peter, D. (2012). "Three-dimensional numerical modeling of sound propagation and scattering in the deep ocean with elastic (shear) bottoms (A)," J. Acoust. Soc. Am. 132, 1973.

Udovydchenkov, I. A., Stephen, R. A., Komatitsch, D., Xie, Z., and Tromp, J. (2014). "Three-dimensional numerical modeling of sound propagation and scattering in the deep ocean with elastic bottoms," paper presented at AGU Ocean Sciences Meeting, Honolulu, February 23-28, 2014.

Williams, C. M., Stephen, R. A., and Smith, D. K. (2006). " Hydroacoustic events located at the intersection of the Atlantis and Kane Transform Faults with the Mid-Atlantic Ridge," Geochem. Geophys. Geosys. 7, doi:10.1029/2005GC001127.

Worcester, P. (2005). "North Pacific Acoustic Laboratory: SPICE04 Recovery Cruise Report, (Scripps Institution of Oceanography, La Jolla, CA.

Yang, Y., and Forsyth, D. W. (2003). "Improving epicentral and magnitude estimation of earthquakes from T Phases by considering the excitation function," Bull. Seismol. Soc. Am. 93, 2106-2122.